

Lossless High-speed Silicon Photonic MZI switch with a Micro-Transfer-Printed III-V amplifier

Jing Zhang
 Photonics Research Group, INTEC,
 Ghent University - imec,
 9052 Ghent, Belgium
 Jingzhan.Zhang@ugent.be

Clemens J. Krüchel
 Photonics Research Group, INTEC,
 Ghent University - imec,
 9052 Ghent, Belgium
 Clemens.Kruechel@ugent.be

Bahawal Haq
 Photonics Research Group, INTEC,
 Ghent University - imec,
 9052 Ghent, Belgium
 Bahawal.Haq@ugent.be

Bozena Matuskova
 EV Group E.Thallner GmbH
 4782 St. St. Florian am Inn, Austria
 B.Matuskova@evgroup.com

Johanna Rimböck
 EV Group E.Thallner GmbH
 4782 St. St. Florian am Inn, Austria
 J.Rimboeck@evgroup.com

Stefan Ertl
 EV Group E.Thallner GmbH
 4782 St. St. Florian am Inn, Austria
 S.Ertl@evgroup.com

Agnieszka Gocalinska
 Tyndall National Institute
 University College Cork
 T12 R5CP Cork, Ireland
 Agnieszka.Gocalinska@tyndall.ie

Emanuele Pelucchi
 Tyndall National Institute
 University College Cork
 T12 R5CP Cork, Ireland
 Emanuele.Pelucchi@tyndall.ie

Brian Corbett
 Tyndall National Institute
 University College Cork
 T12 R5CP Cork, Ireland
 Brian.Corbett@tyndall.ie

Joris Van Campenhout
 IMEC
 Kapeldreef 75
 3001 Heverlee, Belgium
 Joris.VanCampenhout@imec.be

Guy Lepage
 IMEC
 3001 Heverlee, Belgium
 Guy.Lepage@imec.be

Peter Verheyen
 IMEC
 3001 Heverlee, Belgium
 Peter.Verheyen@imec.be

Dries Van Thourhout
 Photonics Research Group, INTEC,
 Ghent University - imec,
 9052 Ghent, Belgium
 Dries.VanThourhout@UGent.be

Roel Baets
 Photonics Research Group, INTEC,
 Ghent University - imec,
 9052 Ghent, Belgium
 Roel.Baets@UGent.be

Gunther Roelkens
 Photonics Research Group, INTEC,
 Ghent University - imec,
 9052 Ghent, Belgium
 Gunther.Roelkens@ugent.be

Abstract—We demonstrate an array of C-band high-speed silicon MZI switches with integrated III-V amplifiers on the imec iSiPP50G platform using micro-transfer printing. The integrated amplifiers exhibit 10 dB optical gain which enables lossless switching and facilitates cross-talk suppression of the switches.

Keywords—Silicon photonic MZI switch; III-V-on-Si amplifier; micro-transfer printing;

I. INTRODUCTION

By leveraging the mature CMOS fabrication facility and the well-established processes, photonic integrated circuits (PICs) can be fabricated on 200 mm or 300 mm wafers in a high-volume and at low-cost. Thanks to the high refractive index contrast and the availability of a variety of high performance passive and active monolithic building blocks (doped Si and Si/Ge components), complex PICs with compact

footprint can be realized for applications in a wide range of fields, e.g. optical interconnects[1], optical computing[2], optical sensors[3], bio-medical instruments[4], LiDARs[5], etc. However, the increase in complexity is always accompanied by additional optical losses, which becomes a significant obstacle in scaling the size and complexity of PICs. Therefore, economical and scalable integrated optical gain elements are desired in PICs. For this, III-V semiconductor integration is required.

Among the explored approaches, die-to-wafer bonding has been attracting great attention in the past decade and has been successfully matured for the manufacturing of commercial products by Intel in recent years. However, this approach relies on a modified process flow of the silicon photonics (SiPh) to accommodate the III-V components, which is a huge capital investment. Such investments should

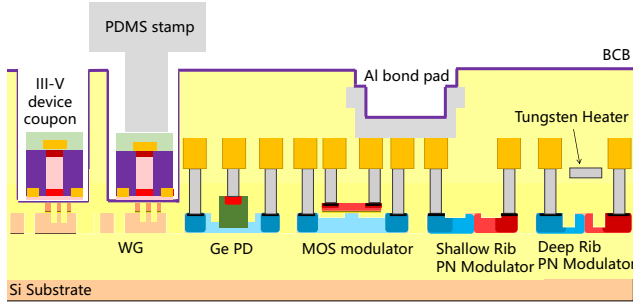


Figure 1. Illustration of the micro-transfer printing of pre-fabricated III-V components in recesses on an advanced SiPh platform.

largely be made again once different III-V materials need to be integrated. In this paper, we demonstrate an approach for the integration of III-V components on an advanced SiPh platform without modifying the established SiPh flow. This approach is based on micro-transfer printing (μ TP) [6]. III-V components that were pre-fabricated in dense arrays on the native III-V epitaxial wafer are released and transfer-printed on a target substrate using an elastomeric Polydimethylsiloxane (PDMS) stamp. To undercut the fabricated III-V devices on the source wafer, a release layer that can be selectively etched is incorporated between the substrate and device layers. The devices are kept in place on the source wafer by photoresist or dielectric tether structures. A thin benzo-cyclo-butene (DVS-BCB) bonding layer is used to achieve high-quality adhesive bonding. After μ TP of the III-V component coupons, only a few simple post-printing steps (DVS-BCB curing and collective wiring of the devices) are needed to finalize the integration. As the III-V component coupons are a few 10s of micron wide, only a local back-end opening on the SiPh wafer is needed to enable the integration of the III-V component on the Si waveguide, as shown in Fig. 1. Following this approach, an array of C-band III-V amplifiers is successfully co-integrated with Si high-speed MZI switches on the imec iSiPP50G platform. The integrated amplifiers show 10 dB optical gain at 100 mA bias current and facilitate optical cross-talk suppression of the switches by 56 dB. High-speed optical switching by routing an externally generated 12 Gb/s data stream through the system array was demonstrated. The on-chip gain provided by the integrated amplifiers is sufficiently high to balance the insertion loss of the Si MZI switch, which enables loss-less optical switching.

II. MICRO-TRANSFER PRINTING OF PRE-FABRICATED III-V AMPLIFIERS

Fig. 2 illustrates the configuration of a single 1×2 Si MZI switch with co-integrated III-V-on-Si optical amplifiers. The MZI switch consists of a pair of $500 \mu\text{m}$ long pin-phase shifters and is controlled through carrier injection by forward biasing the pin-diode[7]. The amplifier region consists of a

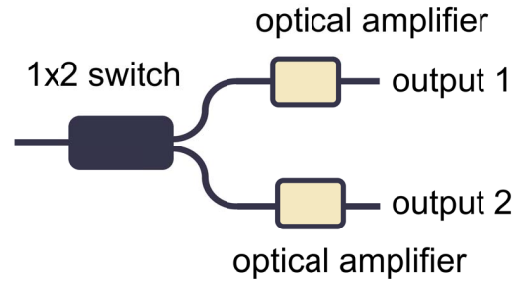


Figure 2. Illustration of the 1×2 switch and optical amplifier system.

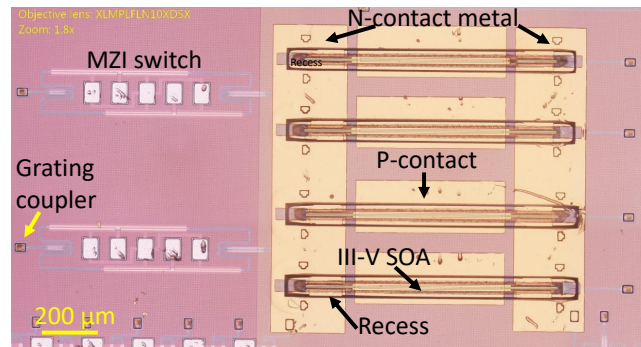


Figure 3. Microscope image of the resulting Si MZI switches with co-integrated III-V amplifiers.

continuous poly-Si/crystalline-Si (160 nm/ 220 nm thick) waveguide with a marker at each side to assist passive alignment in the μ TP process. An additional poly-Si/Si taper structure is used to couple the signal power to the underlying crystalline Si waveguide and vice versa. The back-end layers over the amplifier design were partially removed in the SiPh back-end processes, leaving a $2 \mu\text{m}$ thick SiO_2 cladding layer on the poly-Si layer. The dimensions of the recesses are $80 \mu\text{m} \times 1050 \mu\text{m}$. Therefore the dimensions of the III-V amplifier coupon is defined to be $950 \mu\text{m} \times 45 \mu\text{m}$ long to fit in the recess. The III-V amplifier consists of two $225 \mu\text{m}$ long tapers and a $500 \mu\text{m}$ long straight waveguide. A comprehensive description of the design and fabrication of the III-V SOAs is described in [8]. To enable evanescent coupling between the III-V coupon and the underlying poly-Si/Si device layer, the residual SiO_2 cladding in the recess was removed by a combination of RIE dry etching and HF wet cleaning. As the back-end layer stack is $3.6 \mu\text{m}$ thick (so as the depth of the recess), it is difficult to obtain a uniform and thin DVS-BCB layer in the recess using spin-coating. Therefore spray coating is applied to overcome this issue and the thickness of the spray-coated DVS-BCB layer is controlled to be 75 nm. After a short soft-bake at 150°C the SiPh substrate is ready for the following μ TP process. An X-Celeprint μ TP-100 tool and a PDMS stamp with a

single post of $40\mu\text{m}\times 1200\mu\text{m}$ were used in this work. After transfer printing, an RIE oxygen plasma etching was performed to remove the resist encapsulation layer, followed by a DVS-BCB full curing procedure. The integration was finalized with a standard lift-off process for the metallization of contact pads. The resulting III-V-on-Si PICs are shown in Fig. 3.

III. STATIC CHARACTERIZATION

The optical gain was first characterized on a temperature-controlled stage at 20°C . A Santec510 tunable laser and a HP power meter were used as optical source and to detect the transmitted optical power. Two Keithley 2401 current sources were used to bias the III-V amplifier and the Si MZI switch. In the measurement, the MZI switch was tuned and maintained at maximum transmission, which results in an insertion loss of $\sim 0.3\text{ dB}$ [7]. The tunable laser was swept from 1530 nm to 1580 nm while the on-chip input power is kept at -20 dBm . As shown in Fig. 4 a), a maximal on-chip gain of 10 dB is achieved around 1560 nm and the 3 dB gain bandwidth is over 30 nm at 100 mA. The on-chip gain of the transfer-printed amplifier was obtained by calibrating out the losses introduced by the MZI switch, the grating couplers (GCs) and the fiber-optics. Given a low loss of the Si MZI switch, the demonstrated system can realize loss-less operation and can be a building block in complex transparent routing networks.

To assess the dependence of the system transmission on the switch and amplifier activation state, we tune the switch current from 0 to 4 mA while operating the amplifier under two discrete states associated with current values of 0 and 80 mA. The system transmission at one output port is shown in Fig. 4 b) for light (continuous-wave) at 1550 nm and a waveguide-coupled input power of 0 dBm. We define two switch states: the on-state and off-state at switch currents of 0.2 and 1.1 mA. Although most optical power is transferred to the adjacent output port in the on-state, a fraction of the light leaks into this switch branch. This undesired throughput (optical cross-talk) reaches around -20 dB of the transmitted signal power (Fig. 4 b)). However, in combination with a deactivated amplifier (0 mA driving current), this undesired throughput can be significantly reduced, leading to ultra-low optical cross-talk in the deactivated switch branch. Here we characterize the cross-talk to be reduced by around 56 dB, as illustrated in Fig. 4 b).

IV. HIGH SPEED CHARACTERIZATION

We demonstrate high-speed optical switching by routing an externally generated 12 Gb/s data stream (carrier at 1550 nm) through the system assembly. During this experiment we operate the III-V amplifiers in DC operation while driving the silicon-based switch with a square waveform from an arbitrary-waveform generator (AWG). The repetition rate of the waveform is 15 MHz, suitable for the electronic

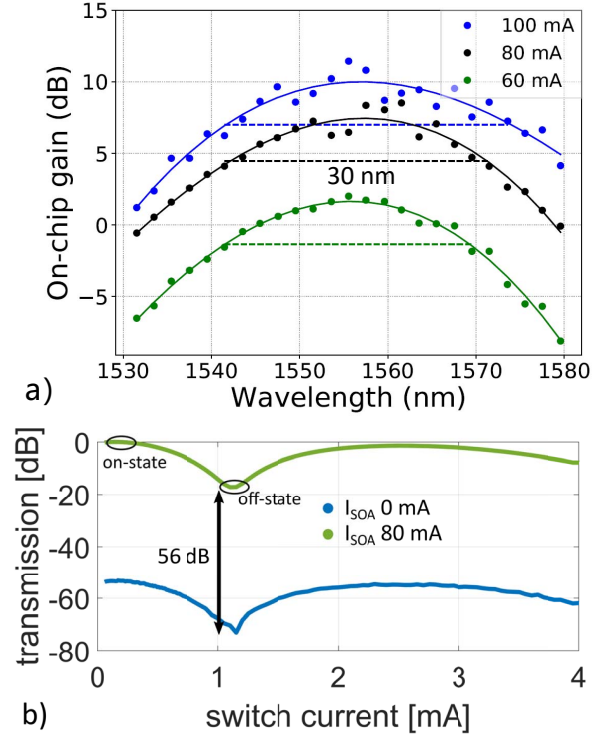


Figure 4. a) On-chip gain spectra for different bias currents. b) Optical transmission vs. switch current. Transmission for SOA current of 0 and 80 mA. The optical cross-talk is reduced by 56 dB with an amplifier operated at 0 mA.

dynamics of the switch. However, higher switching speeds are possible with different driving signals [7] or a carrier-depletion type modulator [9]. In order to maximize the transmission at the switch outputs, we optimize both voltage levels of the square waveform according to DC transmission scans similar to the one presented in Fig. 4 b). With this in mind, we plot the driving signal together with the optical transients of the switch in Fig. 5 a-c). The figure illustrates the system response at different amplification levels corresponding to SOA driving currents of 0 and 80 mA. To simplify matters, the presented optical signals are referenced to the maximum received signal power of the data sets. When switching the 12 Gb/s data sequence (on-off keying, non-return to zero) a similar performance is achieved as can be seen in Fig. 5 d-f) illustrated for a reduced timeframe. The plot exhibits the expected performance and illustrates the aforementioned advantages of the combined technologies. The improvements that result from the integrated amplifier are two-fold: firstly, the amplifiers deliver an increase in signal power at the chip output. Secondly, the amplifier facilitates a larger cross-talk suppression between the power levels at both switch states. The statically characterized improvement of 56 dB is not demonstrated in this dynamic experiment because of the detection limit in the receiver

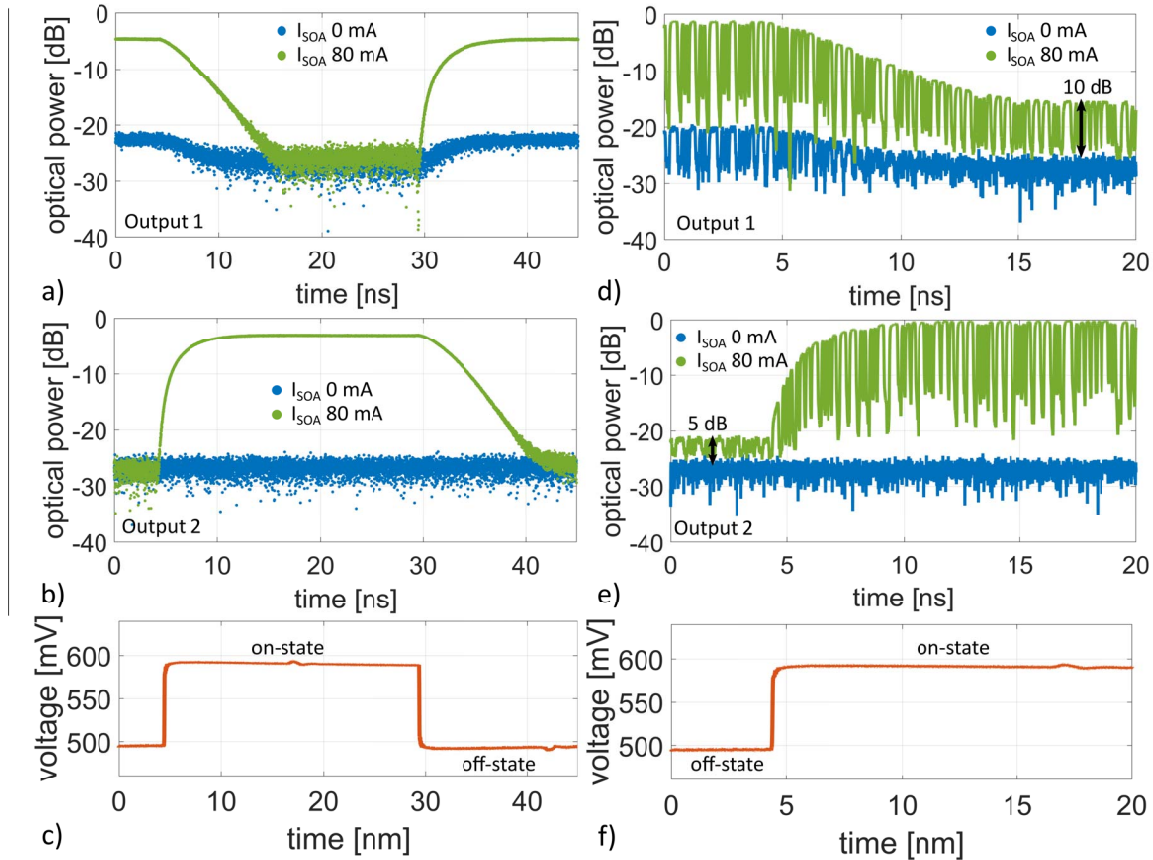


Figure 5. a) and b) Optical transient of switch + amplifier system at different amplifier currents of 0 and 80 mA. c) Electronic driving signal of the switch. d) and e) Optical transient response of system when routing a 12 Gb/s data stream. f) Electronic driving signal of the switch.

stage. In this experiment we can still show an improved extinction ratio of 10 dB and 5 dB at the first and second output respectively.

V. CONCLUSION

This demonstration showcases the back-end-compatible integration of III-V components on an advanced SiPh wafer through μ TP. In fact, a wide range of material films/devices that can be released from the native substrate can be integrated on the target substrate using this approach. The capability of wafer-scale integration in a massively parallel manner that micro-transfer printing brings, allows for high-volume production of complex heterogeneous Si PICs at low cost.

ACKNOWLEDGMENT

This work was supported by the European Union grant 825453 (CALADAN), 814276 (ITN WON), INTERREG-FWVL SafeSide and 713481 (SPICE).

REFERENCES

- [1] H. Mekawey, M. Elsayed, Y. Ismail, and M. A. Swillam, *Optical Interconnects Finally Seeing the Light in Silicon Photonics: Past the Hype*, *Nanomaterials*, 12(3), 485, 2022.
- [2] A. Lugnan, A. Katumba, F. Laporte, M. Freiberger, S. Sackesyn, C. Ma, E.J.C. Gooskens, J. Dambre, P. Bienstman, *Photonic neuromorphic information processing and reservoir computing*, *APL Photonics*, 5, p.020901, 2020.
- [3] A. Tsarev, *Overview of Integrated Optical Sensors Based on Silicon: Forecasts and Results of the Decade*. *Optoelectronics, Instrumentation Data Process* 56:412–30, 2020.
- [4] N. L. Kazanskiy, S. N. Khonina, M. A. Butt, A. Kaźmierczak and R. Piramidowicz, *State-of-the-Art Optical Devices for Biomedical Sensing Applications—A Review*, *Electronics*, vol. 10(8), 973, 2021.
- [5] C. V. Poulton, A. Yaacobi, D. B. Cole, M. J. Byrd, M. Raval, D. Vermeulen, and M. R. Watts, *Coherent solid-state LIDAR with silicon photonic optical phased arrays*, *Opt. Lett.* 42, 4091-4094, 2017.

- [6] B. Corbett, R. Loi, J. O'Callaghan and G. Roelkens, *Transfer printing for silicon photonics*, *Semiconductors and Semimetals*, vol. 99, pp. 43–70, 2018.
- [7] C. J. Krückel, H. Becker, Y. Ban, M. J. R. Heck, J. Van Campenhout, and D. Van Thourhout, *Towards Maximum Energy Efficiency of Carrier-Injection-Based Silicon Photonics*, *IEEE JLT*, vol. 39, no. 9, pp. 2931-2940, 2021.
- [8] B. Haq, S. Kumari, K. Van Gasse, J. Zhang, A. Gocalinska, E. Pelucchi, B. Corbett and G. Roelkens *Micro-Transfer-Printed III-V-on-silicon C-band semiconductor optical amplifiers*, *Laser Photonics Rev.*, vol. 14, p. 1 900 364, 2020.
- [9] A. Liu, L. Liao, D. Rubin, H. Nguyen, B. Ciftcioglu, Y. Chetrit, N. Izhaky, and M. Paniccia, *High-speed optical modulation based on carrier depletion in a silicon waveguide*, *Opt. Express*, vol. 15, no. 2, pp. 660-668, 2021.